

Fragmentation Phase Transitions in Atomic Clusters

III

– Coulomb Explosion of Metal Clusters –

O. Schapiro, P.J. Kuntz, K. Möhring, P.A. Hervieux*,

D.H.E. Gross and M.E. Madjet

Hahn-Meitner-Institut Berlin, Bereich Theoretische Physik,

14109 Berlin, Germany

and

Freie Universität Berlin, Germany

*Institut de Physique, Lab LPMC, 1 Bd Arago, F57078 Metz

Cedex 3, France

Abstract

We discuss the role and the treatment of polarization effects in many-body systems of charged conducting clusters and apply this to the statistical fragmentation of Na-clusters. We see a first order microcanonical phase transition in the fragmentation of Na_{70}^{Z+} for $Z = 0$ to 8. We can distinguish two fragmentation phases, namely evaporation of large particles from a large residue and a complete decay into small fragments only. Charging the cluster shifts the transition to lower excitation energies and forces the transition to disappear for charges higher than $Z = 8$. At very high charges the fragmentation phase transition no longer occurs because the cluster Coulomb-explodes into small fragments even at excitation energy $\epsilon^* = 0$.

1 Introduction: statistical picture

Atomic clusters are especially interesting as a link between macroscopic matter and a single atom. In studying clusters one would usually like to understand how

the material properties evolve with the size of the system. Our special interest is slightly different. We would like to address the very general question of the thermodynamics of finite systems. In this context finite means that the size of the system is of the same order of magnitude as the range of the forces. This imposes an overall correlation within the system which strongly influences its properties. Atomic clusters together with nuclei and gravitational systems are the examples of finite systems.

This paper is the third in a series on "*Fragmentation Phase Transitions in Atomic Clusters*". In the first paper subtitled "*Microcanonical Thermodynamics*" [1] we addressed the most general concepts, and in the second "*Symmetry of Fission of Charged Metal Clusters*" [2] we work out how the material properties influence the fragmentation behavior. In the current work we investigate the influence of charge and polarization effects on the fragmentation of cold and hot Na-clusters and discuss it in light of microcanonical fragmentation phase transitions. The next work planned is on the relation of the fragmentation transition to the commonly known liquid-gas phase transition.

Our overall goal is to calculate the accessible all-possible particle phase space Ω after the fragmentation of a cluster within a given volume. The size of this accessible phase space is restricted by the conservation of the global parameters: mass, charge, total energy and the total angular momentum, which is set to zero in all calculations presented here. In addition there are geometrical constraints: the fragments within the cluster configuration should not overlap after the decay and, moreover, should not be closer than the binding distance of the daughter clusters. In studying a microcanonical system and applying Microcanonical Thermodynamics, we need to define the total volume which is accessible to the fragmenting system. The size of this fixed volume is also one of the geometrical constraints.

In using the MMMC (Microcanonical Metropolis Monte Carlo) model [1, 5] we simulate the accessible phase space at the moment after the fragmentation when the short-range Van-der-Waals forces (and the exchange of atoms) become negligible. This happens at the average surface distances between the fragments of 0.5 to 1 Å.

We simulate the fragmenting configurations within a spherical volume of radius $R_{sys} = r_f * N_T^{1/3}$, where N_T is the number of atoms in the cluster and $r_f = 3.85\text{\AA}$ for Na-clusters. R_{sys} is called the *freeze-out* radius. We want to mention in advance that the results of our calculations are practically independent of R_{sys} , if r_f is kept within reasonable limits. We place all the fragments randomly inside this freeze-out volume under the constraint that the surfaces are further apart than a binding distance $d_b \approx 0.5$ to 1\AA (see Appendix C).

It is also worth noting how the material dependence is included. The ground state binding energies of all possible fragments make up the input to our calculation. For sodium we take the known experimental binding energies for neutral and singly charged clusters up to mass 21 [18, 7]. Since we do not know the binding energies of other clusters we determine them from the liquid drop model. Thus the electronic shell effects are included only for smaller clusters, which are, however, the most relevant to the fragmentation. The weights of individual events (fragmentation configurations) are also dependent on parameters like the Wigner-Seitz radius, moments of inertia of the fragments, and the vibrational frequencies of dimers and trimers. We treat the internal excitations for all the fragments with $N_j \geq 4$ as in the bulk matter where we use the bulk specific entropy (see references [5, 2] for details).

In studying the Coulomb explosion it is important to take polarization effects into account. We do this by calculating the pairwise interactions between the fragments, which we assume to be spherical (See Appendices A and B). The monomers are considered not to be polarizable.

2 Coulomb explosion

The investigation of the stability of charged water droplets goes back to the work of Lord Rayleigh [8] in the year 1882. His ideas were widely applied to similar problems in nuclear and atomic cluster physics. Afterwards, scientists in both of these fields were interested especially in binary fission induced by Coulomb instability as a possible decay channel [9]. In our calculations we allow *all possible* decay chan-

nels of highly charged clusters. This enables us to study the competition between evaporation, fission, multifragmentation, or even total vaporization.

The first experimental evidence for Coulomb instability of clusters was presented by Sattler et al., [10] for small doubly charged clusters. Some experimental techniques for achieving highly charged states for masses $N > 1000$ are discussed in [11]. Here we want to concentrate on masses less than 100 in order to study highly charged states by including the polarization effects and their connection to general questions of thermodynamics in small systems. A comparison with experimental results is a matter for the future.

Generally, the microcanonical phase transition in a small system is signaled by an S-shape in the caloric equation of state $T(E)$ [3, 12, 13], or in other words, a decrease in temperature with growing energy of the system in the transition region: the system cools while it absorbs energy. The thermodynamic temperature T is obtained by calculating the specific entropy, s , from a knowledge of the phase space $\Omega(\epsilon_{tot})$, where $\epsilon_{tot} = E/N$ is the specific total energy:

$$\begin{aligned} \beta \equiv \frac{1}{T} &= \frac{\partial s}{\partial \epsilon_{tot}} \\ s &= \frac{\ln(\Omega(\epsilon_{tot}))}{N}. \end{aligned} \tag{1}$$

For a fixed mass and charge of the cluster, β depends only on the specific excitation energy ϵ^* ,

$$\begin{aligned} \epsilon_{tot} &= \epsilon^* + \epsilon_{binding}(N, Z) \\ \epsilon_{binding}(N, Z) &= \frac{E_{binding}^{N,Z}}{N}. \end{aligned} \tag{2}$$

ϵ_{tot} is the total specific energy available to the fragmenting system and is a globally conserved quantity. ϵ^* is also a conserved quantity, but only for fixed N and Z . In this case, considering the temperature dependence, it is sufficient to look at $T(\epsilon^*)$.

We study the fragmentation of clusters at a fixed volume, as we assume that the motion of complex fragments at short relative distances is dissipative and ergodic.

In order to concentrate on Coulomb and polarization effects, we have examined the statistical fragmentation behavior of the cluster Na_{70}^{Z+} at different charges Z .

Figure 1 shows the fragmentation of Na_{70}^{2+} for a calculation done assuming pairwise interactions between fragments represented by conducting spheres for a minimal surface distance $d_b = 1\text{\AA}$ (See appendices). The left scale shows the three largest masses M1, M2, M3 of the fragments (averaged over all configurations) as a function of the specific excitation energy ϵ^* . We see that at ϵ^* below 0.2 eV the system mostly evaporates monomers. As ϵ^* increases, some heavier particles start to appear, but the most dramatic effect is the abrupt disappearance of the dominating large residue between 0.35 and 0.45 eV. At even larger excitations the cluster decays only into small fragments with masses less than 10. Looking at the thermodynamic temperature T , (the right scale in fig. 1), we see an S-shape in $T(\epsilon^*)$ around $\epsilon^* \approx 0.4$ eV or $T \approx 1200$ K. This S-shape is connected with the disappearance of the large residue and is a typical signature of a microcanonical first order phase transition.

The average masses M1, M2 and M3 give of course only a rough indication about the real mass distribution at any given energy. Figure 2 shows the detailed mass distributions for the same system as in fig. 1 for three individual excitation energies corresponding to just before, during, and after the phase transition. The picture does not show the monomers and does not distinguish between the fragments with the same mass but different charge. Before the phase transition (top panel) Na_{70}^{2+} prefers to evaporate singly charged trimers and Na_9^+ . This is due to the shell effects which we include for small clusters ($N < 21$). For lower excitation energies $0.2 < \epsilon^* < 0.25\text{eV}$ the Na_3^+ channel is much more important than the Na_9^+ channel [2]. The predominance of the trimer channel is consistent with molecular-dynamics predictions for clusters with $4 \leq N \leq 12$, [14] and with the experimental findings in [15]. In our case, however, the occurrence of Na_3^+ cannot be explained just by the least fission barrier, assumed in [15]. We do not restrict the number and type of the outcoming fragments; therefore, the choice of the system to *fission* instead evaporation or multifragmentation in the energy interval $0.2 < \epsilon^* < 0.3$ is not just an energetic, but mainly an entropic effect.

The large residue in figure 2, top, has preferred masses Na_{61}^+ , Na_{67}^+ and Na_{69}^{2+} , corresponding to the emission of exactly one fragment with mass $N = 9, 3$ or a

neutral monomer. Inside the phase transition region (middle panel) we see a very broad distribution of residues combined with two dominating fragments, neutral Na_4 and Na_9^+ . The two available charges go mostly to the large residue and Na_9^+ ; other singly charged small fragments also occur but with much lower probabilities. One also finds channels with doubly charged residues with masses 47 to 61, but this decay channel is even less probable.

After the phase transition (lower panel) no large residue is left and the system decays only into small fragments. The charges prefer to go to two Na_9^+ clusters. Again, other singly charged clusters with masses from 3 to 15 exist, but their probabilities are at least one order of magnitude lower.

Before studying Coulomb explosion we would like to test the importance of polarization effects at different charges. Therefore we compare the conducting spheres (cs) calculation to the point charge (pc) calculation for Na_{70}^{2+} in figure 3. A related question is that of the binding distance d_b between the clusters, because the polarization is strongly dependent on distances. In Appendix C we estimate d_b as 0.5 to 1 Å. In figure 3 we try both d_b values. We see that for $Z = 2$ the thermodynamic temperature, $T(\epsilon^*)$, is insensitive to d_b and polarization. At the same time one can see that the statistical uncertainty in T is about ± 70 K for $\epsilon^* < 0.4$ eV. For larger energies the fluctuations become smaller.

Let us now proceed to higher charges. Figure 4 is the same as figure 1 but for Na_{70}^{8+} . Note the change in temperature and energy scales. The disappearance of the large residue at $\epsilon^* \approx 0.09$ eV coincides with a systematic small S-shape in $T(\epsilon^*)$, indicating a phase transition. For this charge, the signature of the phase transition is of the same order of magnitude as the statistical fluctuations of $T(\epsilon^*)$ in our calculations. For even higher charges the phase transition disappears. For $Z = 8$ the phase transition is shifted significantly towards lower excitation energies and temperatures for the simple reason that the total energy which is available to the fragmenting system is increased by the Coulomb self-energy. Therefore the cluster needs much less additional excitation to undergo the phase transition. The lower transition temperature T indicates that by increasing the excitation energy,

the additionally gained phase space is much less here than for Na_{70}^{2+} . This is quite natural, since the phase space for $Z = 8$ is more strongly restricted by the need to distribute all 8 charges among the small fragments.

Looking in figure 5 at the mass distributions for Na_{70}^{8+} before, during and after the phase transition, we see a slightly different picture from that for Na_{70}^{2+} . We find that at these three energies practically all the fragments, including the residue, are singly charged. In the top and middle panels, the small fragments are predominantly Na_3^+ and Na_9^+ , whereas, just after the phase transition (lower panel), they are Na_7^+ and Na_9^+ . The charged trimers disappear because the system tries to put all available mass into charged fragments. At even higher energies the charged trimers appear again together with neutral fragments.

To illustrate the role of polarization effects, we compare figure 6 ($Z = 8$) with figure 3 ($Z = 2$). The statistical fluctuations make the interpretation somewhat difficult, but two important things are still evident: First, looking at the solid and dotted curves for the conducting spheres interactions (cs) we see that the phase transition, present for $d_b = 1 \text{ \AA}$, is absent for $d_b = 0.5 \text{ \AA}$. It is intuitively clear, that there should be some charge Z which makes the cluster unstable even at $\epsilon^* = 0$ and it explodes into small fragments without any additional excitation. Taking the binding distance $d_b = 1 \text{ \AA}$ this critical charge is $Z = 9$, as we show later. Reducing d_b to 0.5 \AA we allow the fragments to be placed closer, so that attractive many-body polarization forces become even more important and cannot be compensated by repulsive forces any more. This additionally gained energy can be now spent to produce small fragments. The amount of this energy is in this case already sufficient to eliminate the phase transition. (Compare with figure 7.) Performing the same calculation for $d_b = 0.5 \text{ \AA}$ for the point charge interaction (pc) and thereby neglecting the polarization effects, we still see evidence for a phase transition (supported also by appearance and later disappearance of the large residue, as shown in figure 8). The second observation is that, outside the transition region ($\epsilon^* < 0.04 \text{ eV}$ and $\epsilon^* > 0.09 \text{ eV}$), the temperature is systematically higher for conducting spheres than for point charges. For higher excitations, this shift is larger

because of the appearance of neutral fragments, which are especially sensitive to attraction by polarization. Taking polarization effects into account reduces the total Coulomb energy. The system then prefers to put this gained energy into the kinetic energy of the fragments, (See figure 9, lower part.), increasing the temperature of the fragmenting configuration.

Figure 9 shows the partitioning of the energy into Coulomb, kinetic, excitation and binding energy for decaying Na_{70}^{2+} and Na_{70}^{8+} . The energies are normalized with $-E_{tot}$. We see that the Coulomb energy of the decaying configuration is negligible for $Z = 2$, but becomes absolutely dominant for $Z = 8$. Nevertheless, it is not the Coulomb effects but rather the change in mass partition that is significant for the fragmentation phase transition, and this is of the same type for both high and low charge.

Extending now our results to a whole range of charges, we show the caloric equation of state $T(\epsilon^*)$ for charges $Z=0\dots 10$ in figure 10. To help in orientating ourselves in this and the following diagram, we indicate some positions with A, B and C. The dotted curve (A,C) marks the fragmentation phase transition. High charges on the cluster suppress the transition signature and make it disappear for $Z > 8$.

To stress again the significance of the mass partition, figure 11 shows the average mass of the biggest fragment as a function of ϵ^* for charges $Z=0\dots 10$. The dotted curve (A,C) again indicates the fragmentation phase transition. Since, independently of the charge, the transition is signaled by the disappearance of the large residue we can identify the two phases simply by the presence or absence of one dominating large residue in the fragmented configuration. Since this is a micro-canonical first order phase transition, there is also a coexistence region in a certain energy and temperature range (S-shape in $T(\epsilon^*)$). In this region, the fragmentation events can belong to one or both phases but outside it, only to one of them.

The fundamental thermodynamic quantity is not the temperature, but β . (See equations 1.) Figure 12 shows $\beta(\epsilon_{tot})$ in dependence on the *total* available energy, for Na_{70}^{Z+} for charges $Z=2\dots 10$. We see that keeping the total energy ϵ_{tot} constant

and increasing the charge reduces the available kinetic energy and increases β . This is a simple way to see how a *non-energetic change* of the system modifies the temperature.

In this paper we studied the N-body phase space of Na_{70}^{Z+} -clusters as a function of charge Z and excitation energy. We conclude that in the statistical fragmentation process of metal clusters we can see microcanonical fragmentation phase transitions for different cluster charges. We can identify the two phases by the presence or absence of a big residue in the fragment configuration. Very high charges destroy the phase transition and force the cluster to explode into small fragments even at an excitation energy $\epsilon^* = 0$. For Na_{70}^{Z+} this happens for $Z > 8$. The predicted charge and mass distributions in such a decay process might be also accessible experimentally. A question still open is whether a dynamical fragmentation follows the details of the phase space. This is connected to the question as to whether the dynamics is sufficiently ergodic or, in other words, whether an experiment is an equilibrated process. Different methods of exciting or charging the cluster might lead to different results concerning the equilibration condition. If this condition is reached, one should be able to see the signature of a phase transition in a suitable experiment.

Appendix A: Polarization effects in many-body systems and the approximation by the two-body interactions

Coulomb interaction is a long-range interaction which is responsible for the overall correlation of the fragmenting system. This interaction contributes significantly to the total (conserved) energy. In our calculation we consider all the fragments to be conducting and spherical because alkali clusters are metallic even for very small sizes [18]. In a fragmenting many-body configuration the polarization effects are important. It is known how to treat the polarization of two spherical droplets from [16]. Here we address the questions of how to treat polarization effects in a N-body

system and how good the spherical approximation is for very small clusters.

Generally, calculating Coulomb energy of a conducting sphere with charge Z and radius R in presence of a point charge Z_P at distance d from its center we need to evaluate the interaction of an inhomogeneous charge distribution on the surface of the sphere with this point charge Z_P outside. Evaluating E_{coul} by the method of image charges we substitute this complicated interaction by the sum of two point charge interactions: first, Z_P with the charge Z_C in the center of the sphere, and second, Z_P with its image charge Z_I which is at distance d_I from the center of the sphere [17]. The Coulomb energy resulting from the surface charge distribution is exactly equal to the E_{coul} from the image charge method if

$$Z_I = -\frac{R}{d}Z_P, \quad d_I = \frac{R^2}{d}; \quad (3)$$

$$Z_C = Z - Z_I, \quad (4)$$

because then the surface of the sphere is an equipotential surface. This is exactly the condition for the distribution of surface charge on a conducting sphere.

In our case we want to calculate a Coulomb energy of several charged or neutral spherical clusters at close distances. We are going to iterate the image charge method which gives us at every iteration step a series of image charges which keep the surface of each conducting sphere at constant potential. The total interaction energy is the interaction of image charges of each sphere with all image charges in other spheres. Therefore the exact value of E_{coul} can be achieved numerically with any desired accuracy by performing this iteration.

Let us consider for simplicity first the case of only two clusters A and B with positive charges Z_A and Z_B and radii R_A and R_B at a distance d_{AB} of their centers, see figure 13. Neglecting any polarization effects in the 0 iteration step gives the Coulomb energy E_0 as:

$$E_0 = \frac{Z_A Z_B}{d_{AB}}. \quad (5)$$

In the first iteration step (1) we consider that the point charge Z_A induces a negative image charge $Z_{B1}^{(1)}$ on the cluster B, and vice versa. The image charges are at distances d_{A1} and d_{B1} from the centers of clusters A and B and are on the line

connecting both centers.

$$Z_{A1}^{(1)} = -\frac{R_A}{d_{AB}}Z_B, \quad d_{A1} = \frac{R_A^2}{d_{AB}}; \quad Z_{B1}^{(1)} = -\frac{R_B}{d_{AB}}Z_A, \quad d_{B1} = \frac{R_B^2}{d_{AB}}. \quad (6)$$

To account for charge conservation one needs to subtract the charge $Z_{B1}^{(1)}$ in the center of cluster B and $Z_{A1}^{(1)}$ in the center of cluster A. We get for the central charge:

$$Z_{A0}^{(1)} = Z_A - Z_{A1}^{(1)}; \quad Z_{B0}^{(1)} = Z_B - Z_{B1}^{(1)}. \quad (7)$$

The Coulomb energy E_1 after the first iteration step is then:

$$E_1 = \frac{Z_{A0}^{(1)}Z_{B1}^{(1)}}{d_{AB} - d_{B1}} + \frac{Z_{B0}^{(1)}Z_{A1}^{(1)}}{d_{AB} - d_{A1}} + \frac{Z_{A1}^{(1)}Z_{B1}^{(1)}}{d_{AB} - d_{A1} - d_{B1}} + \frac{Z_{A0}^{(1)}Z_{B0}^{(1)}}{d_{AB}}. \quad (8)$$

In the second iteration step we need first to adjust the image charges at positions d_{A1} and d_{B1} , since the charges in the centers were changed.

$$Z_{A1}^{(2)} = -\frac{R_A}{d_{AB}}Z_{B0}^{(1)}; \quad Z_{B1}^{(2)} = -\frac{R_B}{d_{AB}}Z_{A0}^{(1)}. \quad (9)$$

Further, the image charges $Z_{A1}^{(2)}$ and $Z_{B1}^{(2)}$ induce the second order image charges $Z_{A2}^{(2)}$ and $Z_{B2}^{(2)}$.

$$Z_{A2}^{(2)} = -\frac{R_A}{d_{AB} - d_{B1}}Z_{B1}^{(2)}, \quad d_{A2} = \frac{R_A^2}{d_{AB} - d_{B1}}; \quad (10)$$

$$Z_{B2}^{(2)} = -\frac{R_B}{d_{AB} - d_{A1}}Z_{A1}^{(2)}, \quad d_{B2} = \frac{R_B^2}{d_{AB} - d_{A1}}. \quad (11)$$

For the Coulomb energy we get using $d_{A0} = d_{B0} = 0$,

$$E_2 = \sum_{i,j=0}^2 \frac{Z_{Ai}^{(2)}Z_{Bj}^{(2)}}{d_{AB} - d_{Ai} - d_{Bj}}. \quad (12)$$

In every next iteration step n we consider two aspects: 1) The charges in the center have been changed, therefore we need to adjust the image charges $Z_{A1}^{(n)}$ and $Z_{B1}^{(n)}$, and 2) these image charges induce themselves second-order image charges $Z_{A2}^{(n)}$ and $Z_{B2}^{(n)}$, and so on up to $Z_{An}^{(n)}$ and $Z_{Bn}^{(n)}$. For the Coulomb energy we need to account for contributions from all the image charges in sphere A with all image charges in sphere B:

$$E_n = \sum_{i,j=0}^n \frac{Z_{Ai}^{(n)}Z_{Bj}^{(n)}}{d_{AB} - d_{Ai} - d_{Bj}}. \quad (13)$$

We can show [19] that E_n build a convergent sequence of energies. If charges Z_A and Z_B have the same sign then

$$E_0 > E_2 > E_4 > \dots E_n \dots > E_3 > E_1 \quad . \quad (14)$$

Please note that the even subscripts are on the left side the odd ones on the right.

The extension of the method to 3 or any number of conducting spheres is only a bookkeeping problem. Figure 14 shows, for example, the positions of image charges in the second iterations step for the case of three clusters. Let us concentrate on the left picture showing the complete collection of image charges. Besides the image charges on lines connecting the centers, which are represented by circles, we get image charges resulting from the interaction of the first-order images in one sphere with the other two spheres. The positions of these images are shown by triangles. Calculating energy we use equation 13 extending it to the general case by the summation over all the spheres.

It is also clear that this method is valid if some of the conducting spheres are neutral. They are attracted due to polarization by the charged clusters.

Our main aim is to find a representative set of configurations in phase space Ω . For 1000000 configurations with 3 to 4 fragments it is no big problem to calculate the Coulomb interaction exactly. But for most of the excitation energies we need configurations with many more fragments. The exact treatment of the Coulomb energy makes the statistical task unsolvable within a reasonable computation time. Therefore we investigated whether we can separate the many-body interaction into the sum of two-body interactions.

We first concentrate on a three-body case, see again figure 14. Considering only the two-body interactions, right picture, we neglect the image charges symbolized by triangles in the left picture.

We describe the positioning of three clusters by two variables, the distance d_C of the center of the sphere C to the center of mass of A and B and d_{AB} the distance between the centers of A and B. Figure 15 shows the Coulomb energy surface for three Na_{10}^+ clusters. The plateau at the small d_{AB} and d_C is a forbidden area where

the fragments would overlap. Figure 16 is the difference ΔE between the exact three-body interaction and the sum of the two-body interactions. The difference is smaller than 2%. Testing different combinations of masses $N = 10$ and $N = 100$ of the three singly or multiply charged fragments always yields $\Delta E < 5\%$. The same is true for one or two small neutral clusters in the presence of charged ones. This is well within the desired accuracy.

Generally, the polarization part of the total Coulomb energy increases for larger clusters and smaller charges. The polarization part becomes especially dominant for a big neutral cluster in the presence of small charged ones at *very* short distances. In this case the approximation by a sum of two-body interactions gives an arbitrarily large deviation from the exact many-body calculation. In our fragmentation calculation of a charged metallic cluster we *never* get configurations where the whole charge goes into small fragments aside one big neutral residue if the fragments have to be placed at surface distances larger than a binding distance $d_b \approx 0.5\text{\AA}$. Therefore we use the two-body conducting sphere approximation, evaluating the Coulomb energy in the MMMC calculation of metallic cluster fragmentation.

Finally, to illustrate the role of polarization effects we have shown a calculation for the fragmentation of Na_{70}^{2+} and Na_{70}^{8+} in figures 3 and 6. We get systematically lower temperatures for the point charge interaction in comparison to the pairwise conducting spheres interaction. This means that taking the point charge interaction makes a smaller phase space accessible than in the case of conducting spheres.

Appendix B: Polarization effects for dimers and trimers

Most of the fragmentation configurations have many small fragments such as dimers and trimers. It is not obvious that treating dimers and trimers as spheres for calculating polarization effects is a good approximation. In order to clarify this, we calculated the interaction of the Na_3^+ trimer-ion with a charged conducting sphere by means of the diatomics-in-molecules (DIM) method, modified in such a way as

to take into account the electrostatic interaction between the ion and the sphere as well as the mutual polarizabilities[20]. The DIM method yields the potential energy surface of the trimer as a function of the inter-nuclear distances and can correctly describe the dissociation of the trimer-ion into $\text{Na}_2^+ + \text{Na}$ or $\text{Na}_2 + \text{Na}^+$. In the presence of the sphere, the charge distribution in the molecule and the geometrical configuration may alter because of the electrostatic interactions. We found that the energy as a function of distance from the sphere is nearly the same as that calculated from the electrostatic energy alone provided that the charge distribution and geometrical configuration are allowed to relax freely. The energy also depends on the orientation of the trimer, there being two local minima at a fixed distance from the sphere: orientation A, an isosceles triangle having its apex between the sphere and the base, and orientation B, where the apex lies on the far side of the base as seen from the sphere. The energies for these two local minima bracket the electrostatic energy as calculated by treating the trimer as a sphere. Finally, when the trimer approaches too closely to the sphere, it becomes unstable because all of the charge flows onto the nearest atom, which is no longer bound to the neutral dimer.

Figure 17 shows the two orientations A and B of a trimer corresponding to minima in the interaction energies. The curves show the dependence of the Coulomb interaction energy on the distance of the center of mass of the trimer to the surface of the cluster of radius 27 bohr and charge 5. The minimal orientation A is in nice overall agreement with molecular dynamics calculation [14]. The dot-dashed curve corresponds to the interaction between two conducting spheres, where the radius of the trimer-sphere was again taken as $r_{trimer} = r_s 3^{1/3}$. To put this approximation in relation to more simplified solutions, we show figure 18 which is a blow-up of figure 17. The dotted curve is the approximation by point charge interaction for the charge localized in the centers, and the short dashed curve is when considering the large cluster as a polarizable sphere and the trimer as a point charge outside.

This shows the validity of a spherical approximation for calculating the polarization energies for trimers.

For a dimer the situation is even better, since there is only one minimum in

energy for the orientation radial to the cluster. In this case all the polarized charge moves as in the image charge method above.

Of course, considering many-body configurations, the dimers and trimers cannot have the same orientation to all the fragments. Even though we cannot account for the individual orientations because of the demands on computer time, we know at least that the spherical approximation, which is like averaging over all orientations, gives a reasonable result.

Appendix C: The minimal surface distances d_b between the clusters

Another much more important point is the minimal surface distance d_b for the clusters not to be bound to each other. It would be natural to assume that this distance is of the order of magnitude of the sum of the electronic spill-outs [21, 22] of the two interacting clusters. The problem is that spill-out is in general charge dependent and is probably strongly deformed by the presence of another charge outside the considered cluster. Therefore we obtained a rough estimate from the DIM calculation (see Figure 17), which also gives the forces experienced by the three trimer atoms. The calculation break down when the attraction of one of the trimer atoms to the cluster is larger than its binding within the trimer. This minimal distance gives an estimate for the lower limit of d_b as $d_b \approx 0.5$ to 1\AA .

Acknowledgements

We thank the Sonderforschungsbereich SFB 337 of the Deutsche Forschungsgemeinschaft for substantial support and the Freie Universität Berlin for offering us their computation facilities.

References

- [1] D.H.E. Gross, M.E. Madjet, O. Schapiro, *Fragmentation Phase Transitions in Atomic Clusters I, Microcanonical Thermodynamics*, Z. Phys. D **39**, 75-83 (1997)
- [2] M.E. Madjet, P.A. Hervieux, D.H.E. Gross, and O. Schapiro, *Fragmentation Phase Transitions in Atomic Clusters II, Symmetry of Fission of Charged Metal Clusters*, Z. Phys. D in print
- [3] D.H.E. Gross, Rep. Prog. Phys. **53** (1990) 605-658, and earlier work of this author cited there.
- [4] A. Chbihi, D.H.E. Gross, O. Schapiro, S. Salou, and L.G. Sobotka, to be published
- [5] D.H.E. Gross and P.A. Hervieux Z. Phys. D **35**, 27-42 (1995).
- [6] C. Brechignac, Ph. Cahuzac, J. Leygnier, and I. Weiner, Dynamics of unimolecular dissociation of sodium cluster ions, J. Chem. Phys, **90**, 1492 (1989)
- [7] M.M. Kappes, M. Schär, U. Röthlisberger, G. Yeritzian, and E. Schumacher, Sodium cluster ionization potentials revisited: Higher-resolution measurements for Na_x ($x < 23$) and their relation to bonding models., Chem. Phys. Lett. **143**, 251 (1988)
- [8] Lord Rayleigh, Philosophical Magazine, XIV, p.p. 184-186, 1882
- [9] C. Baladron, J.M. Lopez, M.P. Iniguez, and J.A. Alonso, Coulomb explosion of charged jellium clusters, Z. Phys. D **11**, 323 (1989)
- [10] K. Sattler, J. Mühlbach, O. Hecht, P. Pfau, and E. Recknagel, Evidence for Coulomb Explosion of Doubly Charged Microclusters, Phys. Rev. Lett, **47**, 160:163 (1981)
- [11] U. Näher, H. Göhlich, T. Lange, and T.P. Martin, Observation of Highly Charged Sodium Clusters, Phys. Rev. Lett. **68**, 3416:3419 (1992)

- [12] A. Hüller, Finite size scaling at first order phase transitions?, *Z. Phys. B* **95**, 63 (1994).
- [13] D.H.E. Gross, *Microcanonical Thermodynamics and Statistical Fragmentation of Dissipative Systems - the Topological Structure of the N-body Phase Space*, *Phys. Rep.* **279**, 119-202 (1997)
- [14] R.N. Barnett, U. Landman, and G. Rajagopal, Patterns and Barriers for Fission of Charged Small Metal clusters, *Phys. Rev. Lett* **67**, 3058 (1991)
- [15] C. Brechignac, Ph. Cahuzac, F. Carlier, M. de Frutos, and J. Leygnier, Simple metal clusters, *Z. Phys. D* **19**,1-6 (1991)
- [16] H.J. Krappe *Z. Phys. D* **23**, 269 (1992)
- [17] J. D. Jackson, *Classical Electrodynamics*, Chapter 2, John Wiley & Sons, New York (1975)
- [18] C. Brechignac, Ph. Cahuzac, F. Carlier, and J. Leygnier, Photoionization of Mass-Selected K_n^+ Ions: A test for the Ionization Scaling Law, *Phys. Rev. Lett.*, **63**, 1368 (1989)
- [19] O. Schapiro, PhD-Thesis, Freie Universität Berlin, Fachbereich Physik, 1997
- [20] P.J. Kuntz, A DIM model for sodium cluster-ions interacting with a charged conducting sphere, *Mol. Physics*, **88**, 693 (1996)
- [21] C. Yannouleas and U. Landman, *Chem. Phys. Lett.* **210**, 437 (1993)
- [22] C. Yannouleas and U. Landman, *Phys. Rev.* **B51**, 1902 (1995)

Figure 1: Na_{70}^{2+} : Average three largest masses M1, M2, M3 (left scale) and the thermodynamic temperature (right scale) as a function of specific excitation energy ϵ^* . $d_b = 1\text{\AA}$, pairwise conducting spheres interaction.

Figure 2: Na_{70}^{2+} : Mass distributions for different specific excitation energies ϵ^*

Figure 3: Na_{70}^{2+} : Thermodynamic temperature $T(\epsilon^*)$ for different d_b values and conducting spheres (cs) versus point charge (pc) Coulomb interactions.

Figure 4: Like figure 1 for Na_{70}^{8+} .

Figure 5: Like figure 2 for Na_{70}^{8+} .

Figure 6: Like figure 3 for Na_{70}^{8+} .

Figure 7: Like figure 4 for $d_b = 0.5\text{\AA}$.

Figure 8: Like figure 7 for point charge interactions.

Figure 9: Partition of the total available energy for fragmenting Na_{70}^{2+} and Na_{70}^{8+} .

Figure 10: Na_{70}^{Z+} : Caloric equation of state $T(\epsilon^*)$ for charges $Z=0\dots 10$. The dotted curve indicates the fragmentation phase transition.

Figure 11: Na_{70}^{Z+} : Average mass of the biggest fragment in dependence on ϵ^* for charges $Z=0\dots 10$. The dotted curve indicates the fragmentation phase transition. The Points A, B and C indicate the corresponding places in figure 10.

Figure 12: Na_{70}^{Z+} : $\beta(\epsilon^*)$ for charges $Z=2\dots 10$.

Figure 13: First iteration steps for evaluation of Coulomb interaction energy by the method of image charges in case of two conducting spheres A and B with charges Z_A and Z_B .

Figure 14: The second iteration step for evaluation of Coulomb interaction energy by the method of image charges for three conducting spheres A, B and C with charges Z_A, Z_B and Z_C .

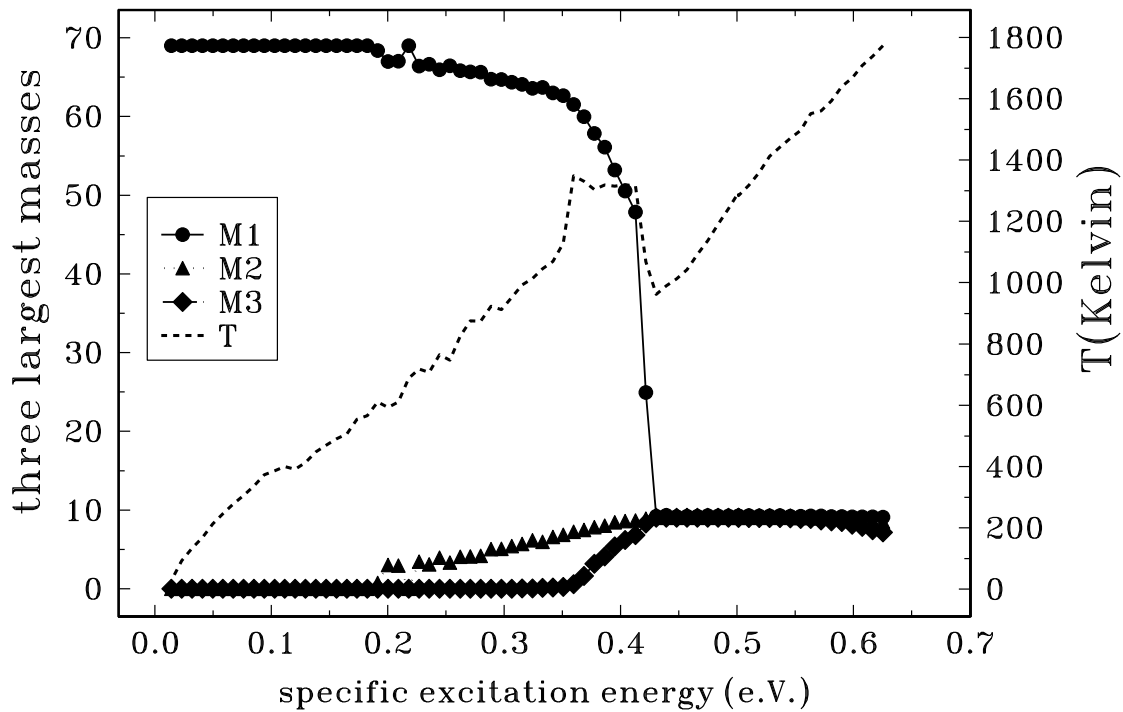
Figure 15: Exact three-body Coulomb energy E of three spherical conducting clusters with mass $N=10$ and charge $Z=1$ as a function of different relative positions, see text, Appendix A.

Figure 16: Difference ΔE between E , figure 15 and the sum of the two-body interactions of three spherical conducting clusters with mass $N=10$ and charge $Z=1$ as a function of different relative positions, see text, Appendix A.

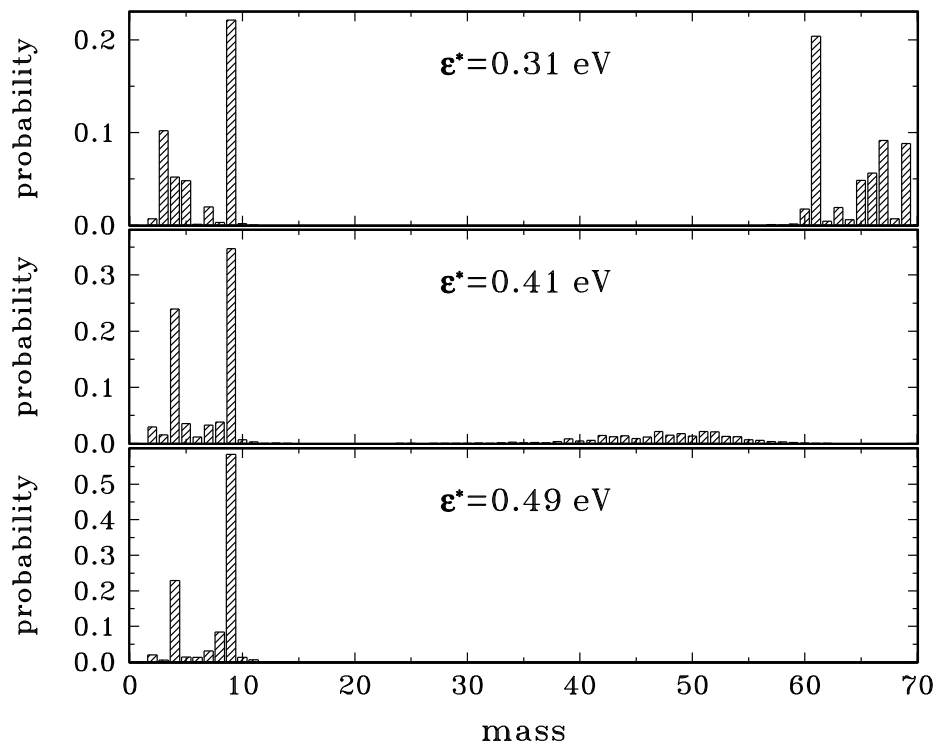
Figure 17: Coulomb energy for a charged sodium trimer in a Coulomb field of a spherical cluster with radius 27 bohr, $Z=5$ for two orientations A and B, see text, Appendix B. The dot-dashed curve is a spherical approximation of a trimer.

Figure 18: The three curves from figure 17 are shown together with two other approximations for Coulomb energy: Dotted curve considers both, a sphere and a trimer having fixed point charges in their centers. Dashed curve shows the point charge approximation just for the trimer in presence of conducting sphere.

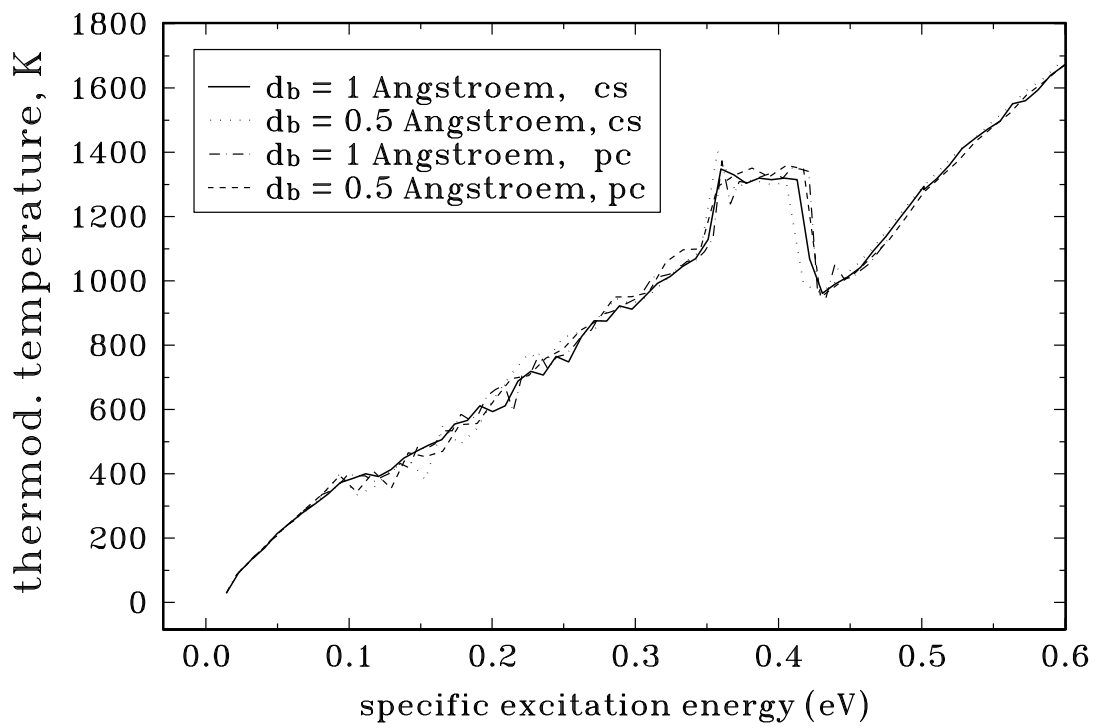
Na²⁺₇₀



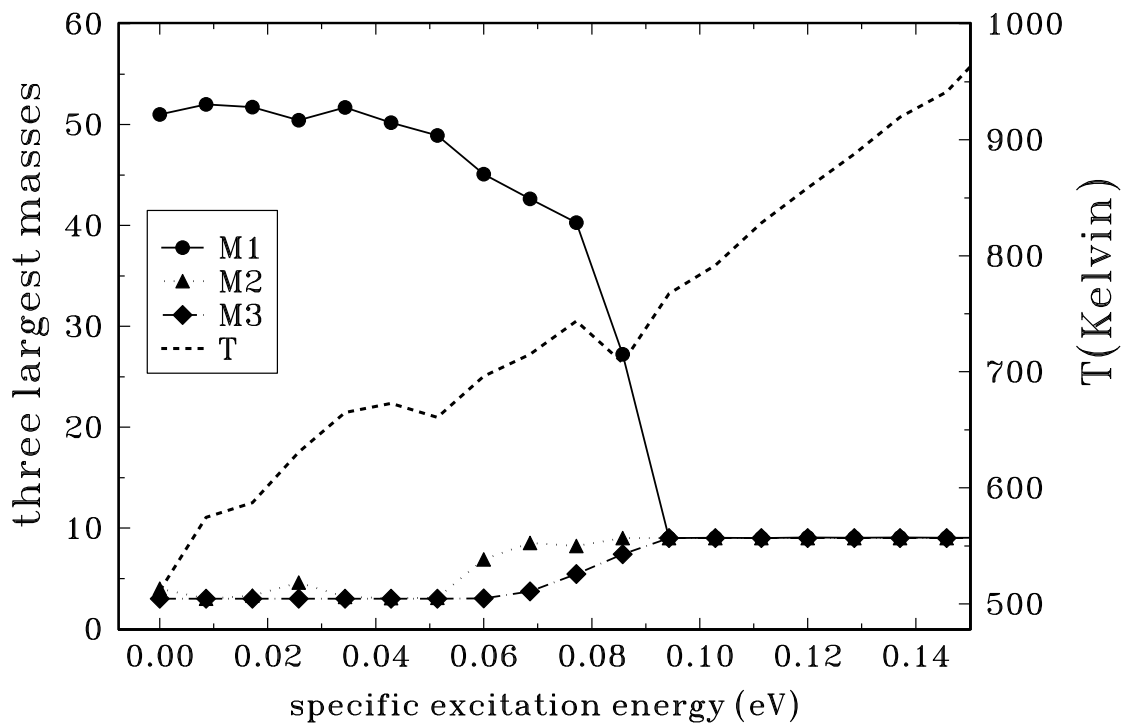
Na_{70}^{2+}
without neutral monomers



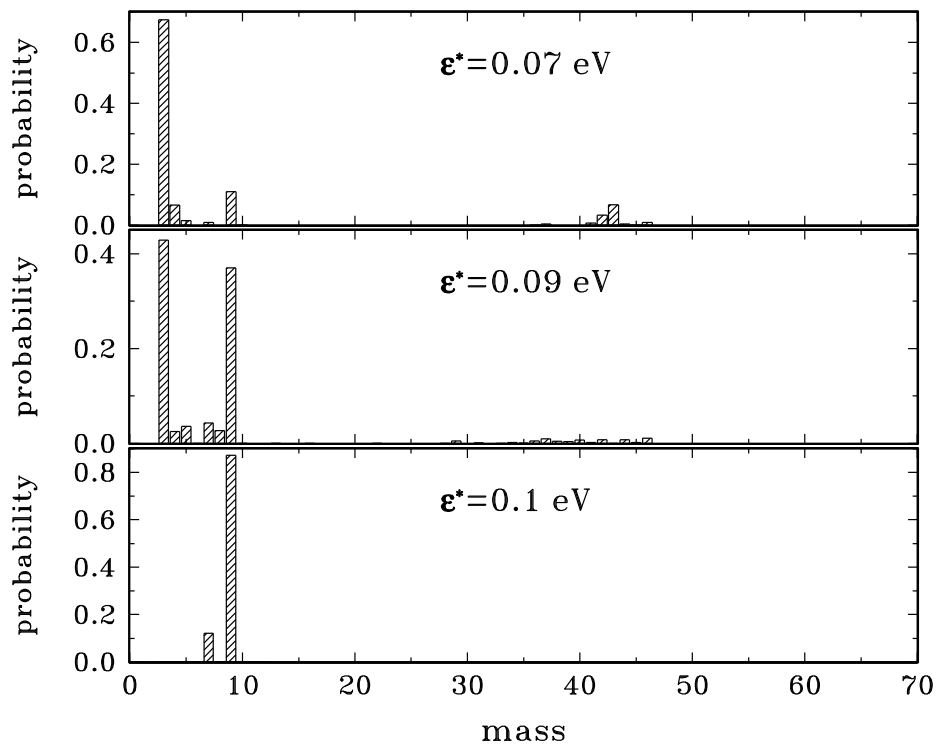
Na²⁺₇₀



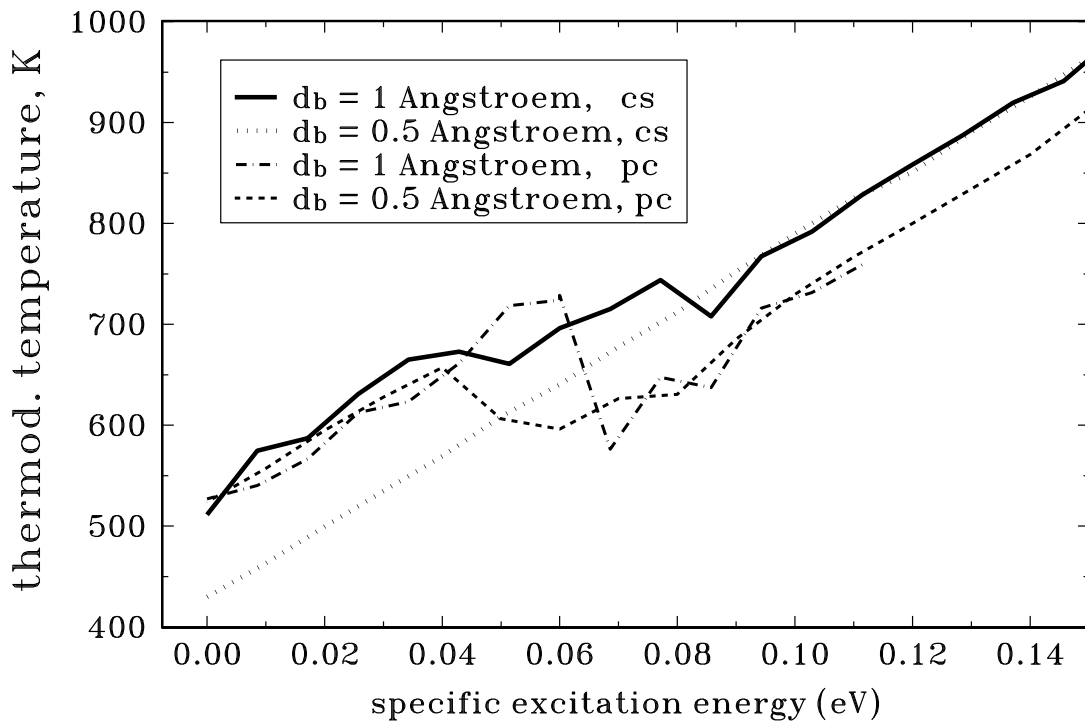
Na⁸⁺₇₀



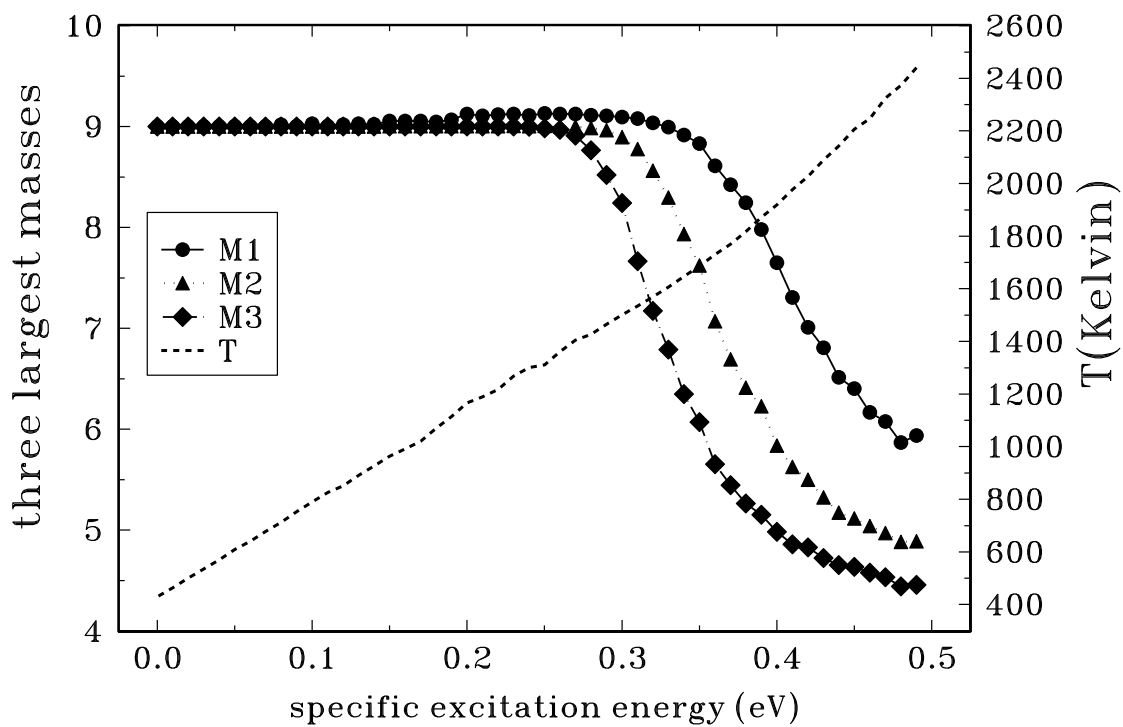
Na_{70}^{8+}
without neutral monomers



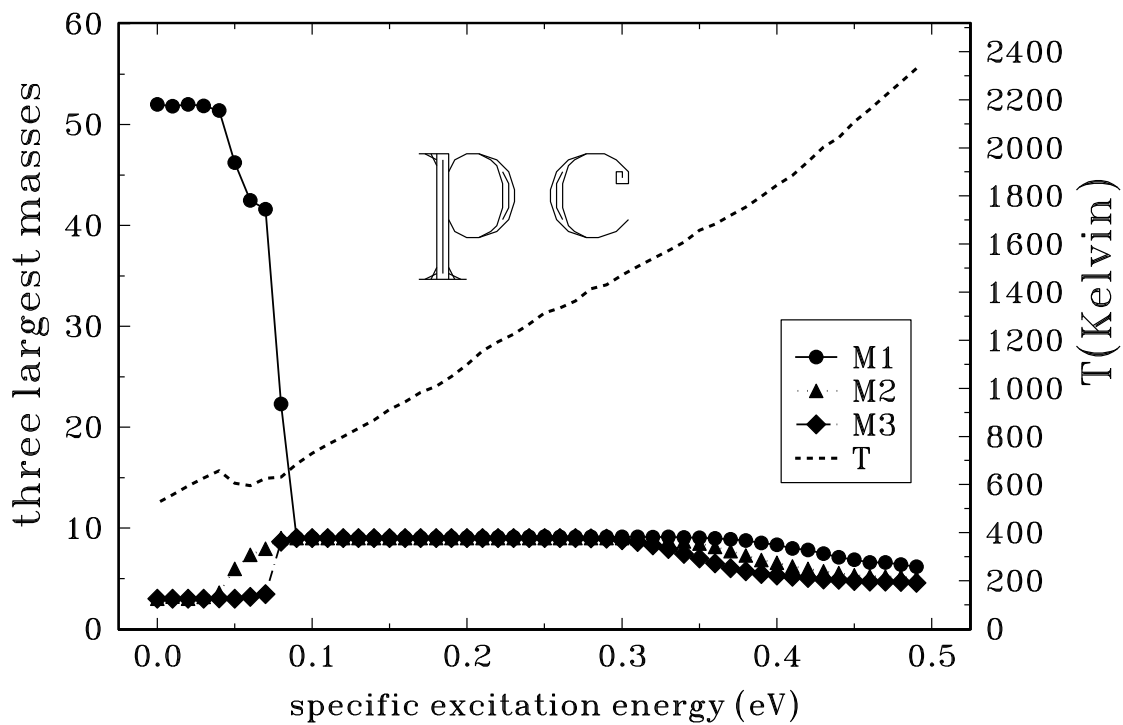
Na⁸⁺₇₀

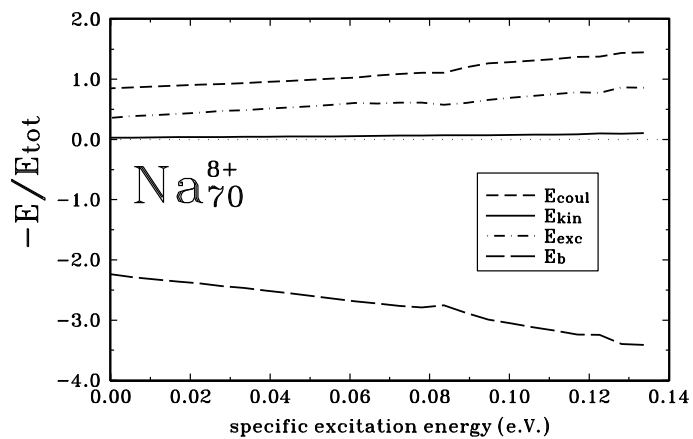
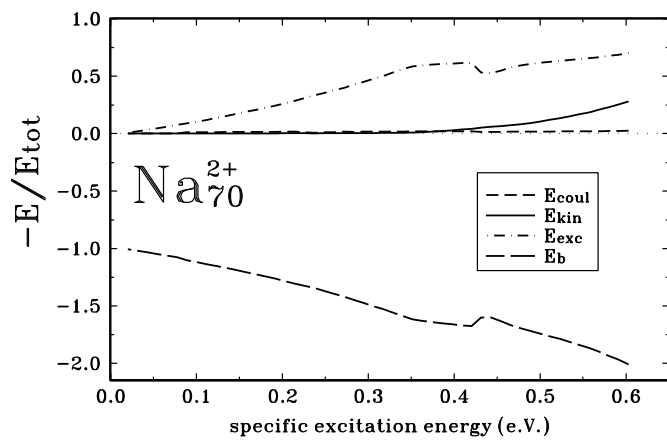


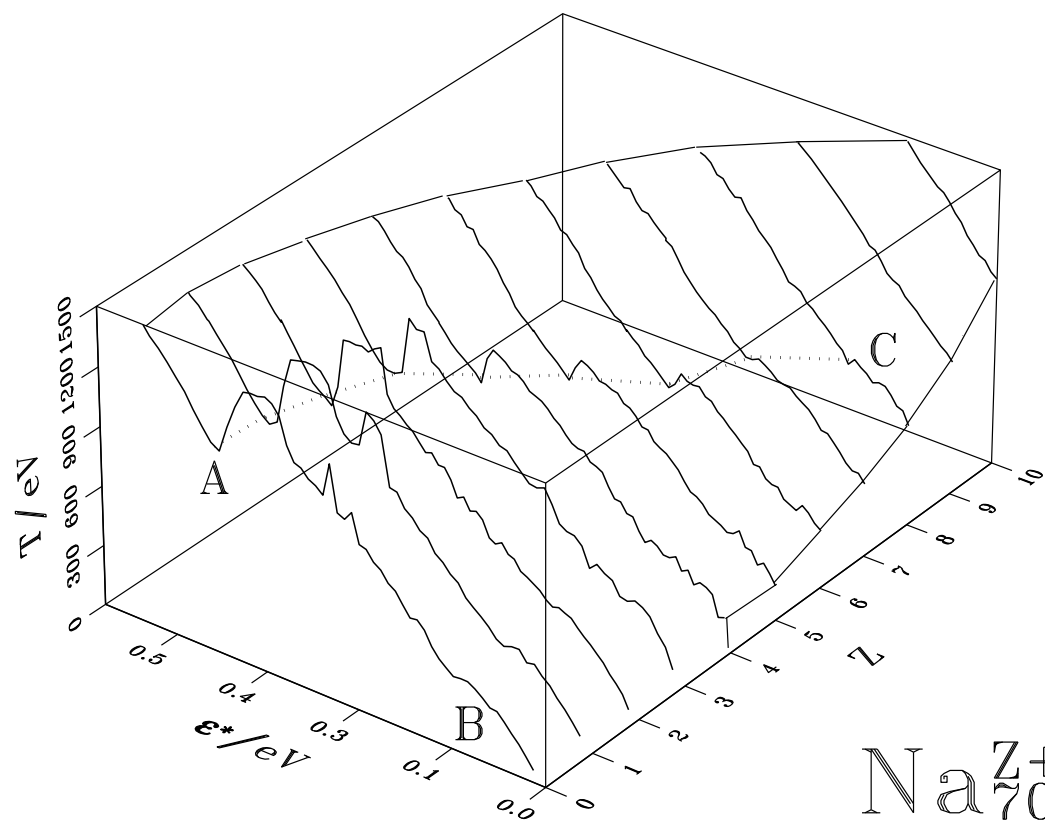
Na₇₀⁸⁺, d_b = 0.5 Angstroem



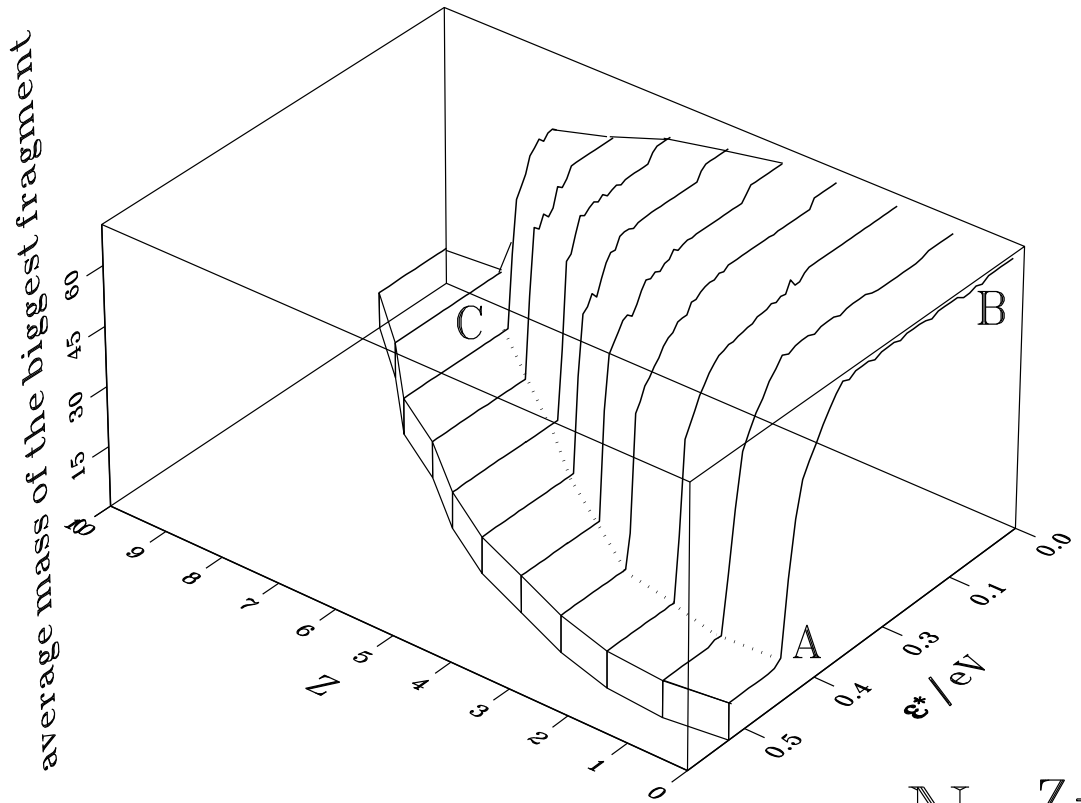
Na₇₀⁸⁺, d_b = 0.5 Angstroem





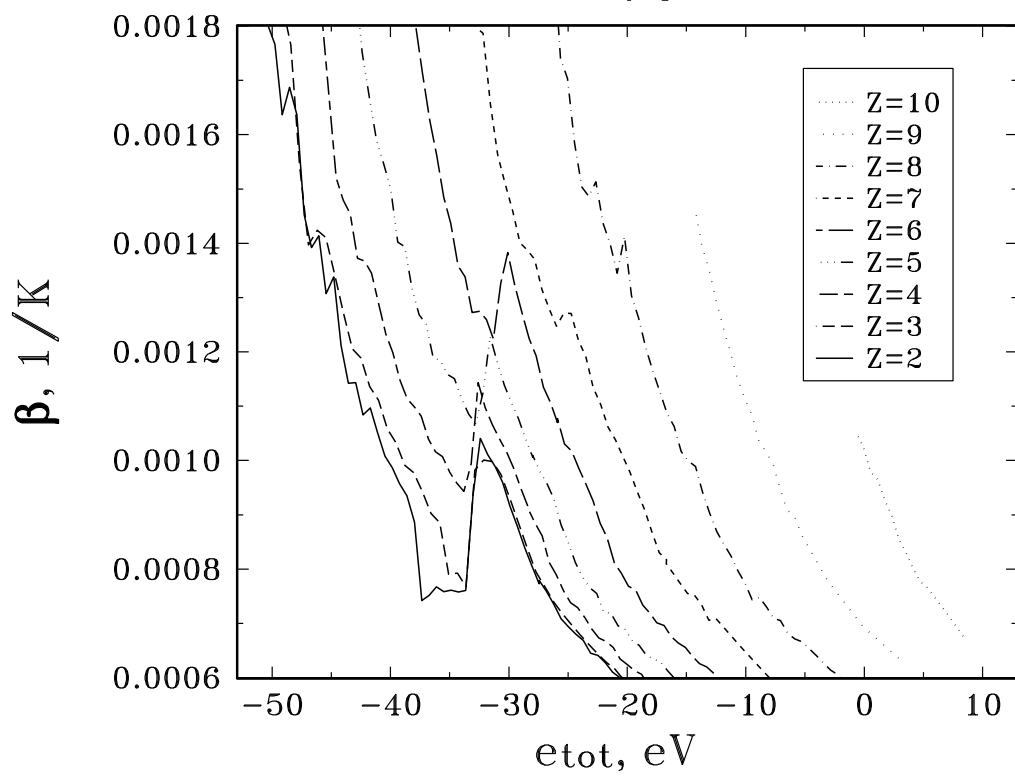


NaZ_{70}^+

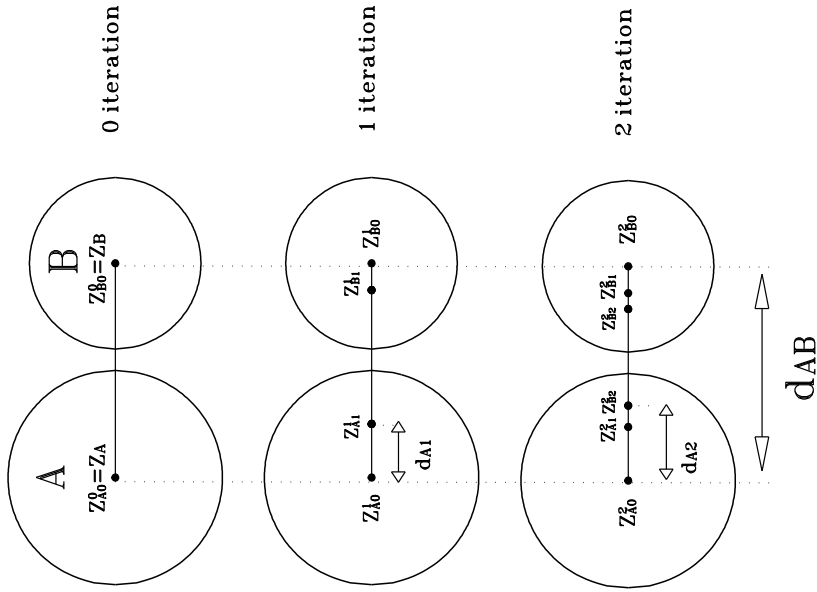


Na_{70}^+

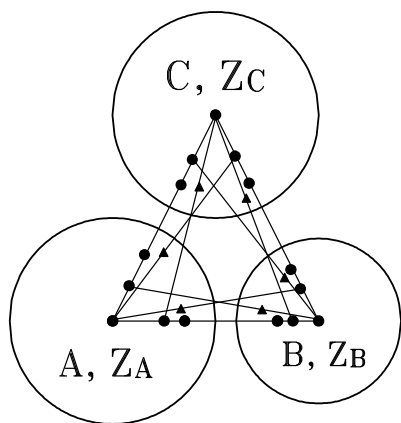
Na_{70}^{Z+}



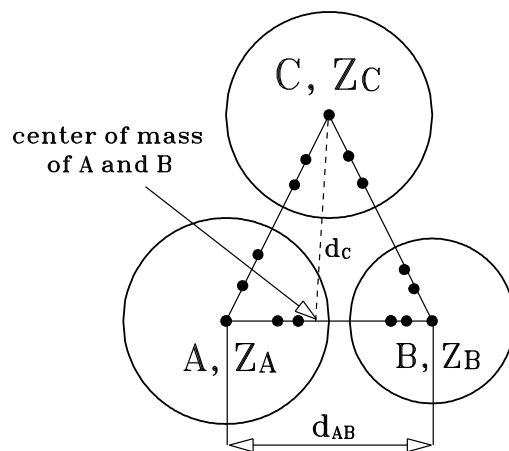
R_A, Z_A R_B, Z_B



second iteration step

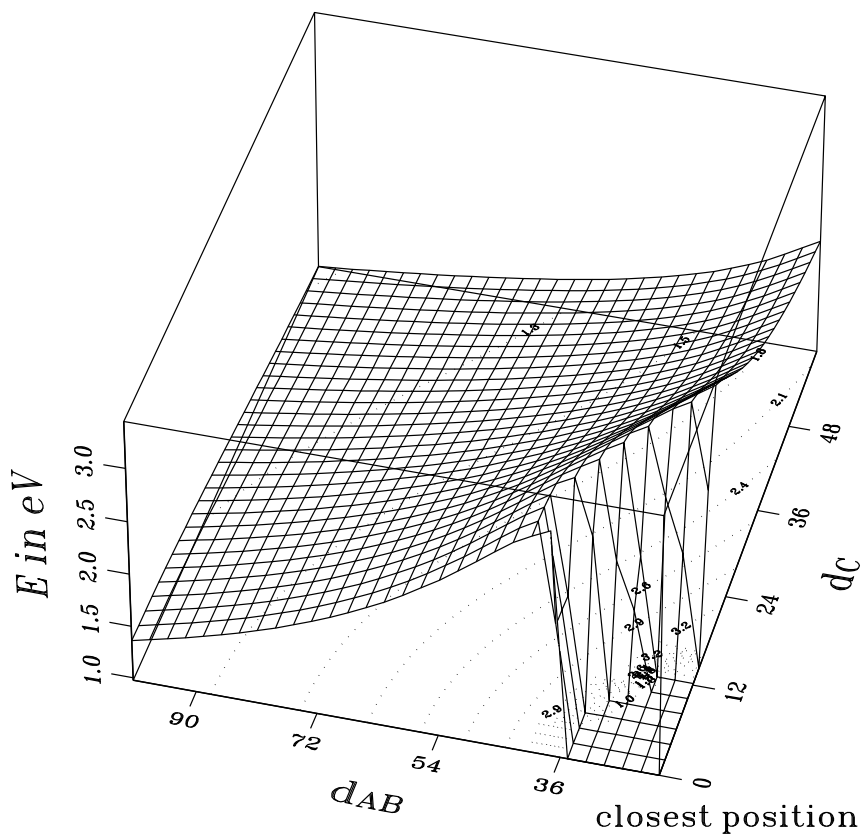


complete
collection of image charges



pairwise
interactions of the spheres

three clusters with $N=10$ atoms, $Q=1$



three clusters with N=10 atoms, Q=1

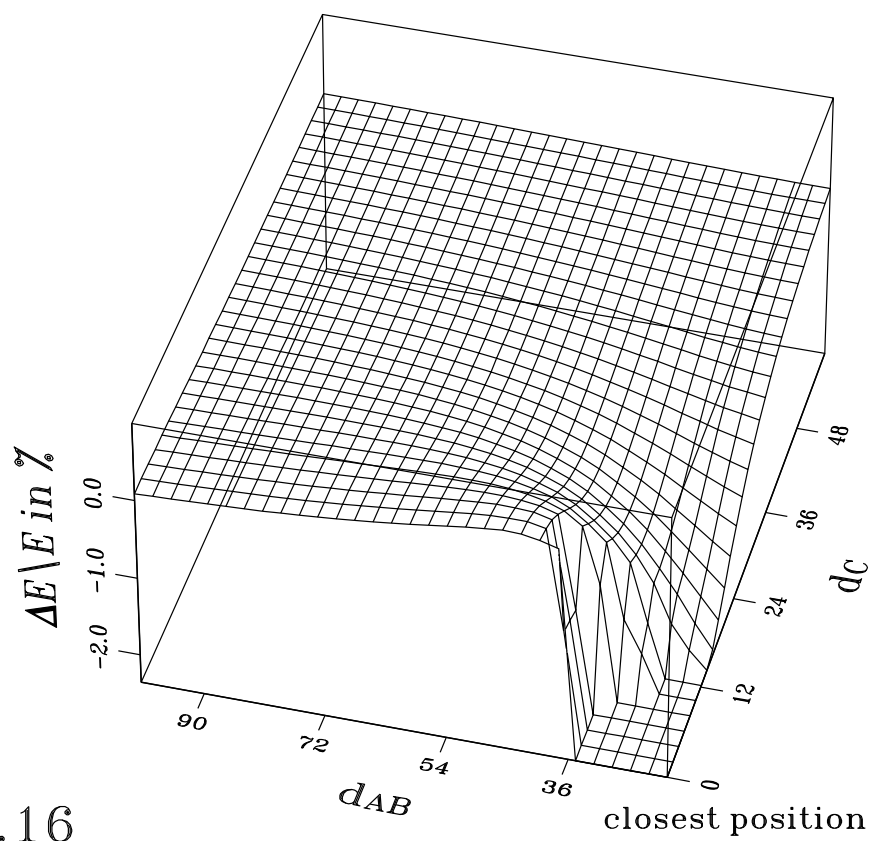


fig.16

